General Disclaimer

One or more of the Following Statements may affect this Document

- This document has been reproduced from the best copy furnished by the organizational source. It is being released in the interest of making available as much information as possible.

- This document may contain data, which exceeds the sheet parameters. It was furnished in this condition by the organizational source and is the best copy available.

- This document may contain tone-on-tone or color graphs, charts and/or pictures, which have been reproduced in black and white.

- This document is paginated as submitted by the original source.

- Portions of this document are not fully legible due to the historical nature of some of the material. However, it is the best reproduction available from the original submission.

NASA CR-144914

DESIGN AND EVALUATION OF THIN METAL SURFACE INSULATION FOR HYPERSONIC FLIGHT

By Robert C. Miller and Alexander M. Petach

JUNE 1976

Prepared under Contract No. NAS1-13606 by

HUGHES HELICOPTERS Division of Summa Corporation
Culver City, California

for

NATIONAL AERONAUTICS AND SPACE ADMINISTRATION

CONTENTS

	Page
SUMMARY	1
INTRODUCTION	1
SYMBOLS AND UNITS	4
PRELIMINARY DESIGN	6
Design Philosophy	6
Minimum Weight Design	8
Insulation Characteristics	8
Heat Transfer Parametrics	10
Thermal Design Optimization	13
INSULATION COMPONENT SELECTION	14
Designs Selected	15
FABRICATION AND EXPERIMENTAL TESTS	17
Fabrication	17
Emissivity Tests	18
Oxidation Tests	19
Structural Tests	20
Erosion/Impact Tests	22
Thermal Conductivity Tests	22
Samples for Hypervelocity Tunnel Test	25
INSTALLATION ON AN AERODYNAMIC SURFACE	26
General Considerations	26
Venting of Insulation	27
Joining of Adjacent Insulation Sections	27
PRODUCTION COSTS	29
CONCLUSIONS	30
RECOMMENDED APPLICATIONS	30
RECOMMENDED STUDIES	31
APPENDIX A: STRUCTURAL DESIGN ANALYSIS	33
APPENDIX B: THERMAL SHORT ANALYSIS	43
Effect of Weld Population on Insulation Thickness	45
REFERENCES	47

DESIGN AND EVALUATION OF THIN METAL SURFACE INSULATION FOR HYPERSONIC FLIGHT

By Robert C. Miller and Alexander M. Petach

SUMMARY

An all-metal insulation has been studied as a thermal protection system for hypersonic vehicles. Key program goals included fabricating the insulation in thin packages which are optimized for high temperature insulation of an actively cooled aluminum structure, and the use of state-of-the-art alloys. The insulation was fabricated from 300 series stainless steel in thicknesses of 0.8 to 12 mm. The outer, 0.127 mm thick, skin was textured to accommodate thermal expansion and oxidized to increase emittance. The thin insulating package was achieved using an insulation concept consisting of foil radiation shields spaced within the package, and conical foil supports to carry loads from the skin and maintain package dimensions. Samples of the metal-insulation were tested to evaluate thermal insulation capability, rain and sand erosion resistance, high temperature oxidation resistance, applied load capability, and high temperature emittance.

INTRODUCTION

An all-metal insulation has been developed as a thermal protection system for hypersonic vehicles such as the space shuttle and a proposed Mach 8 cruise vehicle. The metal insulation concept was originally developed to protect the interior of helicopter hot gas ducts. An all-metal insulation, consisting of metal wool packaged in foil was studied under a NASA contract (ref. 1) as an alternative to the ceramic reusable surface insulation which is the baseline thermal protection system for the space shuttle. The metal insulation systems are potentially more flexible, more resistant to impact and erosion, and as light as the impact and strain sensitive ceramic systems. Figure 1 shows that the thermal conductivity of metal insulation compares very favorably with other high performance insulations.

Under the present contract, an all-metal system was studied as a surface insulation for use over the actively cooled aluminum structure of a proposed Mach 8 cruise vehicle. An active cooling system for a hypersonic vehicle, using the available hydrogen fuel as a heat sink, may require augmentation by a high-temperature surface insulation to reradiate part of the

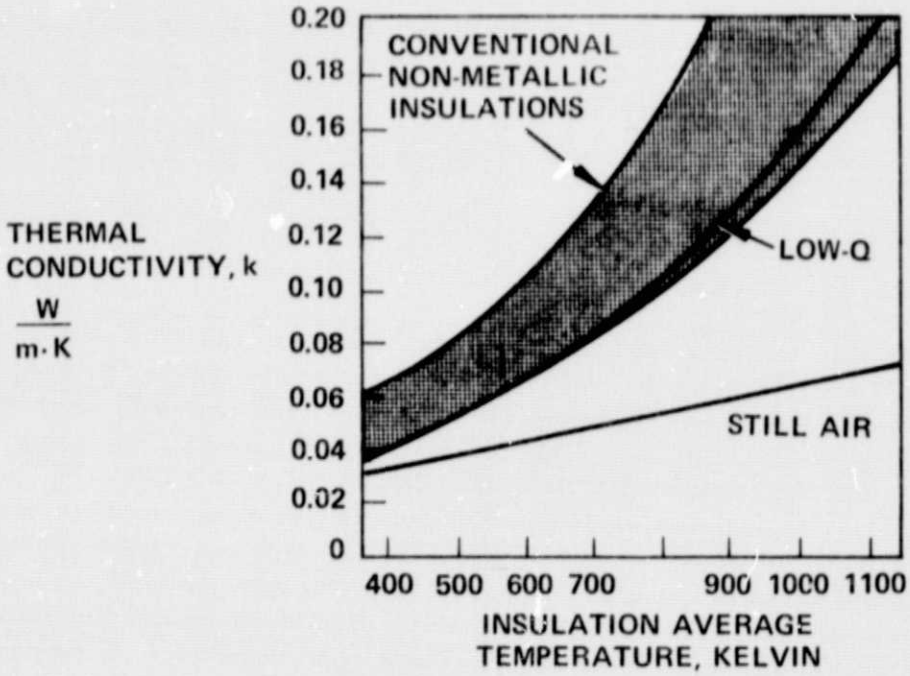

Figure 1.—Thermal conductivity of LOW-Q compared to conventional non-metallic insulations.

incident heating so that the primary structure temperatures can be limited to the allowable range for aluminum. For efficient use of the active cooling capacity, the surface insulation should be very thin, establishing a large temperature gradient between the outer surfaces of the insulation and the cooled structure. The objectives established for this study include design and construction of metal insulations in a thickness range of 0.25 to 10 mm, using state-of-the-art alloys capable of sustaining temperatures up to 1200°K.

The key elements in an insulation package which would meet the study goals include an aerodynamic skin capable of accommodating thermal expansion and resisting impact and erosion; a low-conductivity internal structure to support the skin, maintain the package dimensions and carry air-loads; and the insulation packaged within the resulting system. The insulation concepts were fabricated into laboratory specimens and a series of environmental tests were performed to evaluate thermal insulation, erosion resistance, oxidation resistance, and load capability. The study also addressed manufacturing methodology, attachment to the vehicle structure, and venting of the insulation package interior. A sketch of the evolved configuration is shown in figure 2a and photographs of typical test specimens are shown in figure 2b.

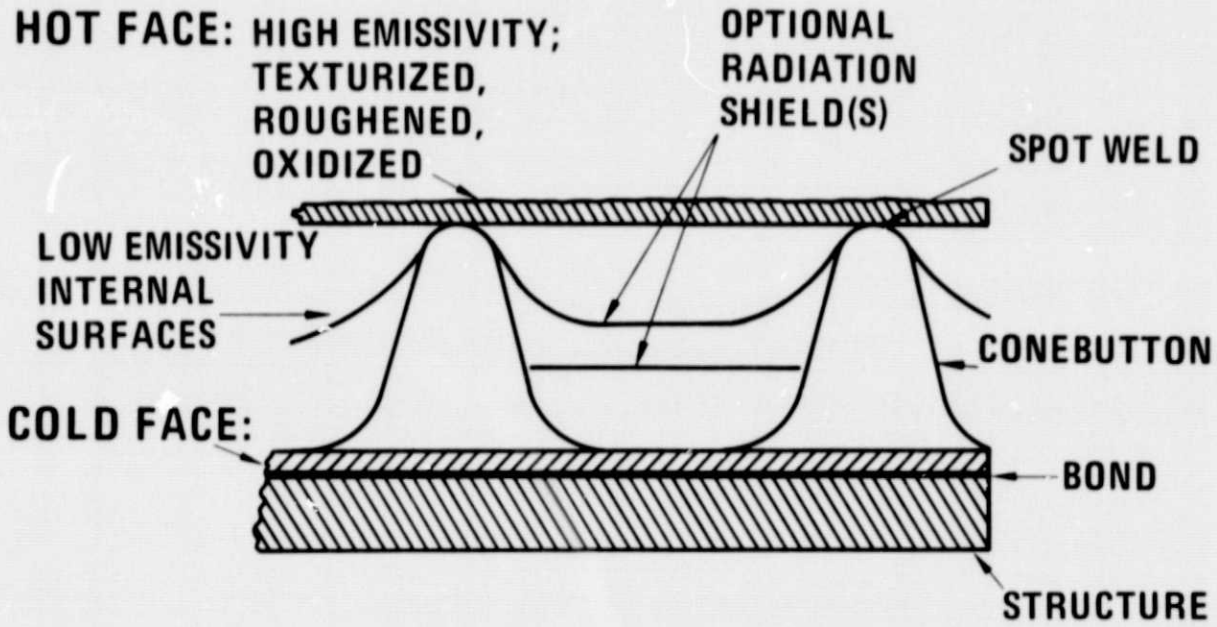

(a) Insulation resulting from study

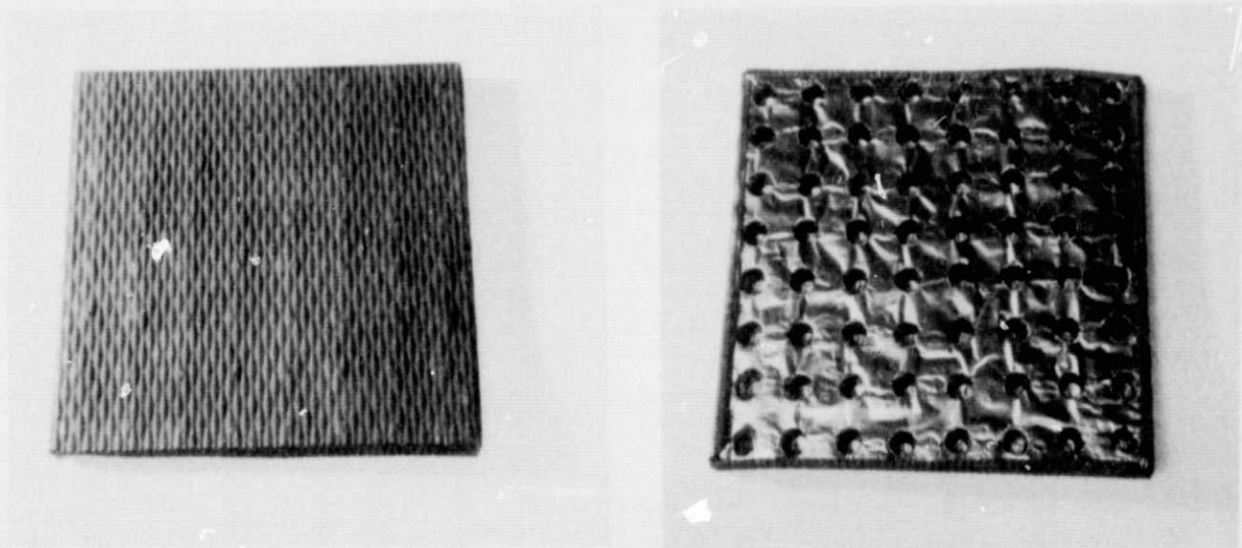

(b) Photographs of thin metal insulation configuration 5 (127 mm squares)

Figure 2

SYMBOLS AND UNITS

A	heat transfer area, m^2
A	annular area of cone wall, mm^2
A_b	area of annular base, mm^2
A_N	area of individual weld nugget, mm^2
A_o	Area of apex, mm^2
a	shorter side of rectangular array, mm
a	$\equiv (A_b - Ao)/\ell = (A - Ao)/x$, mm
b	longer side of rectangular array, mm
D	$\equiv Eh^3/(1 - \nu^2)$, dimensionless
d	weld nugget diameter, mm
dT	differential temperature normal to heat flow, K
dx	differential distance normal to heat flow, mm
E	modulus of elasticity, GN/m^2
f_t	weld allowable tensile strength, MN/m^2
h_h	wall thickness of cone, mm plate thickness, mm
h_c	air conductance, $w/m^2 \cdot K$
h_r	radiation conductance, $w/m^2 \cdot K$

h_t conductance of insulation with thermal shorts, $w/m^2 \cdot K$

K $\equiv -k/(T_b - To)\, Ao/\ell$, W

k thermal conductivity, $w/m \cdot K$

k_i thermal conductivity of insulation without thermal shorts, $w/m \cdot K$

k_{ss} thermal conductivity of stainless steel, $w/m \cdot K$

ℓ height of conebutton, m

m even integers (2, 4, 6, etc.), dimensionless

N number of welds per square meter, m^{-2}

n number of shields, dimensionless

n $\equiv A_b/A_o$, dimensionless

P_2 negative pressure differential, MN/m^2

Q heat flow, kW

q uniform loading, kN/m^2

T_b temperature of conebutton base, K

T_o temperature of conebutton apex, K

t thickness, mm

w weight per unit area, kg/m^2

x distance from cone apex towards base, mm

x_m $\equiv m\pi b/2a$, dimensionless

x_t equivalent thickness of insulation with thermal shorts, mm

ϵ emissivity, dimensionless

ν Poisson's ratio, dimensionless

ω skin deflection, mm

PRELIMINARY DESIGN

Design Philosophy

A design review lead to the following conclusions:

1. The most efficient thermo-structural system, from inspection of previous analysis (ref. 1) is a structural packaging of a low conductivity, low density, metal insulation where structural loads are primarily carried by the packaging system.

2. Metal insulation is not a homogeneous system.

3. In general, a thermally efficient insulation is not an efficient structure. When structural requirements are combined with thermal excellence, a heavy insulation results.

4. Emphasis should be placed on a skin structure design that will withstand pressure loads with minimum deformation, and with a minimum number of thermal shorts.

5. The outer skin should have a high emissivity outer surface and a low emissivity inner surface to limit heat input to the system.

6. High emissivity may be obtained by:

   - Rough surface
   - High emissivity coating
   - Oxidized surface
   - Combination of rough surface and oxidation

7. A rough oxidized surface formed by the parent skin material is preferred for the following reasons:

   - Coating is not necessary
   - Lower sensitivity to abrasion
   - Lower maintenance
   - Lower cost

The three specific insulation thicknesses shown in table 1 were selected for study to cover the full range required by the program. The general design criteria which were met are summarized in table 2 and the specific design conditions are given in table 3.

TABLE 1. – THICKNESSES STUDIED

Thin (mm)	Nominal (mm)	Thick (mm)
0.25	1.0	10.00

TABLE 2. – DESIGN CRITERIA

- 1200 K maximum temperature
- Minimum distortion under load
- Accommodates thermal expansion
- Minimum thermal shorts
- Designed to reradiate aerodynamic heat
- Adequate venting
- No gas flow in insulation
- Impact and erosion resistant

TABLE 3. — DESIGN CONDITIONS

Parameter	Value	Parameter	Value
Outer skin max. temp.	1200 K	Free stream mach number	8.0
Insulation cold face temp.	366 K	Dynamic pressure	20.7 to 69.0 kN/m^2
Average insulation temp.	780 K	Surface pressure pulsations	± 13.8 kN/m^2
Altitude	24.4 km	Insulation space max. internal pressure	± 34.5 kN/m^2

Minimum Weight Design

An optimum weight insulation system was defined from a review of the components and their respective variables as shown in table 4.

The definition of each component in terms of its respective variables was performed using an iterative approach. A concomitant inspection of structural and thermal properties was necessary and the heat transfer parametrics presented in following sections of this report were developed to support this area of design.

Insulation Characteristics

LOW-Q, Type W, Type S and Type S-1, which were candidates for the thin metal insulation systems, are schematically shown in figure 3.

TABLE 4. – FACTORS INFLUENCING INSULATION WEIGHT

Component	Variables
Skin	1. Thickness 2. Points of support 3. Material 4. Shape of skin plane
Insulation	1. Density 2. Thermal conductivity 3. Thickness 4. Thermal shorts 5. Maximum service temperature 6. Radiant and conductive heat
Supports	1. Configuration 2. Population 3. Heat shorts 4. Producibility

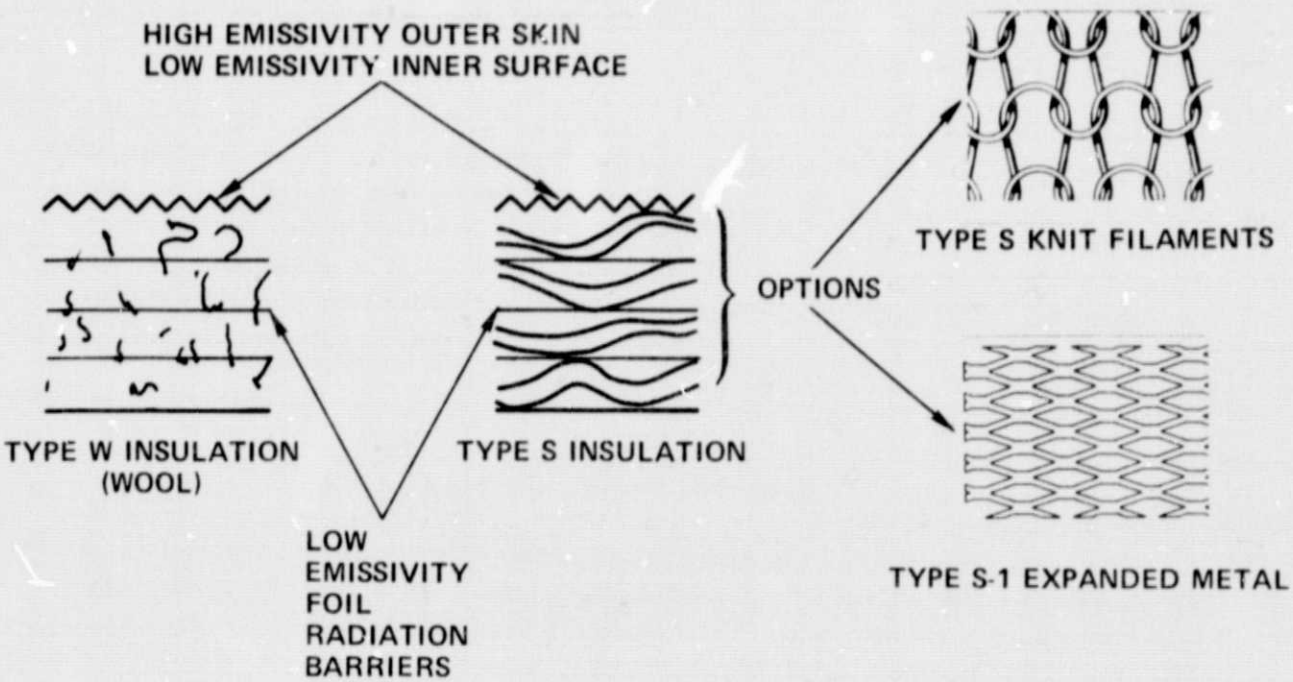

Figure 3. – Schematics of LOW-Q type W, S, and S-1 all metal insulations.

LOW-Q Type W Insulation. — Type W is a metal wool insulation whose filaments can be selected in the range of 0.0254 to 0.127 mm diameter for high temperature service. The large filament diameter deemed necessary for the insulation required herein dictates that radiation barriers be placed in the insulation laminate, since the wool population would not be sufficiently opaque. Stainless steel wools were employed for a similar heat shield study (ref. 1), where high temperature service was required. Low temperature environments may effectively use other metal wools, such as aluminum.

Recent experiments (ref. 3) performed by Hughes demonstrated that Type 304 and 307 stainless steel filaments up to 12 microns in diameter could be ignited with a match flame in the presence of a service air jet and support combustion until the air jet was removed. The test results indicate that the use of steel or stainless steel filaments of less than 25 micron diameter should be avoided in high temperature, high air velocity environments, unless appropriately packaged.

LOW-Q Type S Insulation. — This metal insulation is composed of layers of knit filaments which are displaced by crimping and separated by foil radiation barriers to provide thermal performance which closely parallels Type W systems. Features of this system are: low cost, use of commercial materials, and no increase in insulation weight. The use of metal filaments typically larger in diameter than those present in metal wools effectively eliminates the problem of insulation combustion, should the outer skin become penetrated.

LOW-Q Type S-1 Insulation. — Type S-1 employs expanded metal foil in place of the wire filament-shield system described for Type S. Expanded foil is a commercial product and may be obtained in a range of thickness. A minimum stretch (expansion) of the foil and a maximum upset (thickness dimension) permits this material to perform as both a stand-off and a radiation barrier. Corrugated ribbons of foil are considered a derivative of expanded metal foil. Such ribbons were used in making the two thickest of the five configurations fabricated for this program.

Heat Transfer Parametrics

The heat flow through a metal insulation system is a summation of many interacting modes of heat transmission. This limits the rigorous analytical assessment of a design and, ultimately, a design must be experimentally verified. Parametric analysis is almost mandatory to focus detailed study in the most productive areas.

Initially, qualitative analysis was used to assist subsequent quantitative analysis. Heat flow through an insulation was reviewed in terms of classic modes of transfer and the methods available to limit the heat flow, as illustrated in table 5.

TABLE 5. – HEAT LEAKS AND WAYS TO MINIMIZE THEM

Item	Type of Heat Leak Thru Insulation	Assessment of Methods to Minimize Heat Leak
1	Conduction through entrained gas	Little control may be exercised short of reducing gas pressure to level where insulation particle spacing is less than the mean free path of the entrained gas molecules
2	Metal conduction	Design employs a minimum of contact area from element to element
3	Natural convection of entrained gas	Controlled easily by the spacing of physical elements of the insulation matrix
4	Radiation from hot to cold face	a. Can be reduced by multiple radiation shields b. Number of radiation shields can be reduced by using low emissivity materials

A second qualitative review was directed at the attenuation of radiant heat transmissions, since this mode contributes largely to the heat flow through an insulation. The results of this review are given in table 6.

TABLE 6. – RADIATION ATTENUATION METHODS

Item	Radiation Reduction Method	Design Constraints
1	Radiation Barriers	a. Thin insulation places practical limits on the number of shields b. Insulation weight increases with with many barriers c. Increase in metal thermal shorts with increasing number of shields
2	Low Emissivity Shields	a. Cost b. Ability of low emissivity material to withstand high temperature c. Comparison of one low emissivity shield with many high emissivity shields
3	No Shields	a. Use low emissivity surface on both internal faces of the insulation blanket b. Use high population density insulation matrix (like metal wool) to inherently provide a number of shields to eliminate emissivity effect c. Shields are not needed to control convection for gaps less than 10 mm

Thermal Design Optimization

A quantitative parametric analysis was performed which served as the basis for subsequent configurations. An analytical comparison of the full range of insulation thickness studies is presented in table 7 for no radiation barriers (zero radiation attenuation), an infinite number of radiation barriers (100 percent radiation attenuation), and a selected near optimum design. The optimum design varies from a zero number of radiation shields to several, and their number is guided by the heat transfer attenuation benefits they represent.

TABLE 7. — INSULATION AS AFFECTED BY RADIATION

Thickness, mm	Insulation Thermal Conductivity, k = W/m · K (average temperature = 780 K)			Radiant Heat Flux, Percent of Total	
	Zero Radiation Attenuation*	100% Radiation Attenuation	Optimum Design	Zero Radiation Attenuation	Optimum Design (Shields)
	A	B	C	(A - B) 100/A	(C - B) 100/C
Thin: 0.25	0.07	0.06	0.07	14	14 (no shields)
Nominal: 1.02	0.10	0.06	0.06	40	~0 (1 gold shield)
Thick: 10.2	0.50	0.06	0.09	88	33 (1 gold, 2 SS shields)

*Based on realistic emissivities, not black-body conditions.

Optimization of the insulation system is seen to depend heavily on the benefits of radiation attenuation as a function of primary variables such as weight, thickness, and complexity. The beneficial influence of radiation shields for heat flow attenuation in the thicker insulation is evident from examination of the radiant and conductive heat flow. Thin insulations generally benefit little from the addition of radiation shields, and an optimum configuration was defined (specimen no. 1) which does not have radiation barriers.

INSULATION COMPONENT SELECTION

The insulation system that was developed is summarized in table 8 where component candidate options and the selection rationale are presented.

TABLE 8. – SELECTION OF INSULATION COMPONENTS

Component	Candidates	Selection	Rationale
Hot Outside Skin	• Commercially textured • Micro-corrugated	Commercially textured 0.127 mm thick	• Commercially available • Erosion resistant • Accommodates thermal growth • Omni-directionally stiff • Impact tolerant
LOW-Q Insulation Elements	• Foils (Type S-1) • Wool (Type W) • Mesh (Type S)	Foils (Type S-2)	• Commercially available • Combined stand-off and radiation shields • Minimum cost and weight • Not combustible
Insulation Thickness Control	• "Conebuttons" • Grommets • Foil beams • Columns	"Conebuttons" (0.0254 mm walls)	• Best structure • Low weight • Low thermal short • Weldable • Can be made in strips
"Conebutton" Geometry	• Cones • Pyramids • Pyramids	Cone with 3.175 mm APEX 25° full angle	• Optimized structure • Manufacturable • Provides welding access
Cold Inside Skin	• Flat foil • Textured foil • Screen	Flat foil	• Minimum cost • Minimum weight • Most easily fabricated

Designs Selected

A total of fifty (50) candidate designs were examined and five (5) configurations were selected for fabrication and experimental study. A summary of design variables that were encompassed in the selected configurations are presented in table 9.

TABLE 9.—SUMMARY OF DESIGN VARIABLES

Item	Description	Selected Value
1	Thickness	0.25, 1.0, 10.0 mm
2	Number of Radiation Shields	0, 1, 3
3	Emissivity	Stainless Bright = 0.3 Steel: Oxidized = 0.7 Gold: 0.05
4	Heat Flux Range	8 to 225 kW/M^2 (28:1 spread)
5	Typical Thermal Conductivity	0.058 W/m · K

The characteristics of the selected designs are summarized in table 10.

Laboratory test specimens were prepared for thermal, structural and erosion study based on the configurations presented in table 10.

TABLE 10. – CHARACTERISTICS OF SELECTED DESIGNS*

Item	Parameter	Description	Units	Configurations				
				1	2	3	4	5
1	t	Thickness	mm	0.25	1.02	1.02	10.16	10.16
2	w	Weight	kg/m^2	1.01	1.21	1.01	2.21	2.21
3	n	Number of Shields	-	0	1	0	3	3
4	ϵ	Shield Emissivities	-	-	0.05	-	0.7/0.05/0.7	0.7/0.7/0.7
5	h_c	Air Conductance**	$W/m^2 \cdot K$	227.0	57.0	57.0	6.0	6.0
6	h_r	Radiation Conductance**	$W/m^2 \cdot K$	43.0	3.0	43.0	3.9	17.0
7	$h_c + h_r$	Combined Conductance**	$W/m^2 \cdot K$	270.0	60.0	100.0	9.0	23.0
8	Q/A	Heat Flux*	kW/m^2	225	50	83	8	19
9	k	Thermal Conductivity	$W/m \cdot K$	0.07	0.06	0.10	0.09	0.23

*Based on Design Conditions of table 5.
**Conductance, h, is related to thermal conductivity, k by the relationship h = k/t, where t is the thickness of the insulation.

FABRICATION AND EXPERIMENTAL TESTS

Twenty-six (26) insulation specimens were produced for various experimental evaluations as shown in table 11.

TABLE 11. – TEST SPECIMEN SUMMARY

Number of Specimens	Test Purpose	Description
5	Emissivity and Thermal	30.5 cm square 2 thermocouples on middle shield
3	Mechanical	12.7 cm square
8	Rain and sand erosion	2.5 cm by 5.1 cm 20° and 40° impact angles
10	Langley Research Center Tunnel	12.7 cm square 2 thermocouples each: Hot and cold faces and middle shield

Fabrication

Internal support is provided by Hughes' "conebuttons." These supports are formed integral with the back face sheet up to a nominal insulation thickness of 5 mm and formed in strips for the thicker insulation. Separate fabrication of each conebutton followed by insertion in a back face sheet is judged to be practical for insulation systems of greater thickness than 10 mm.

The texturized outer stainless steel skin was roughened by sand-blasting on its external face and was oxidized to obtain a high emissivity surface ($\epsilon = 0.9$, ref. 4).

Packaging of the "sandwich" insulation required 35 modifications to achieve desired thermal and manufacturing qualities. The successful designs are packaged in a proprietary manner to form the final insulations.

Insulation panels or blankets are nominally limited in width to commercial stainless steel sheet stock, which is available in 0.9 to 1.32 meters. These panels may be joined by welding to permit a larger basic width, should this be required.

Emissivity Tests

A Mikron model 56 infrared thermometer was used to obtain metal surface emissivity. The emissivity test data shown in figure 4 indicates that temperatures higher than 1200 K are required for at least 1 hour to oxidize the surface enough to obtain high emissivity. The emissivity of the oxidized surfaces are close to the prediced value 0.70.

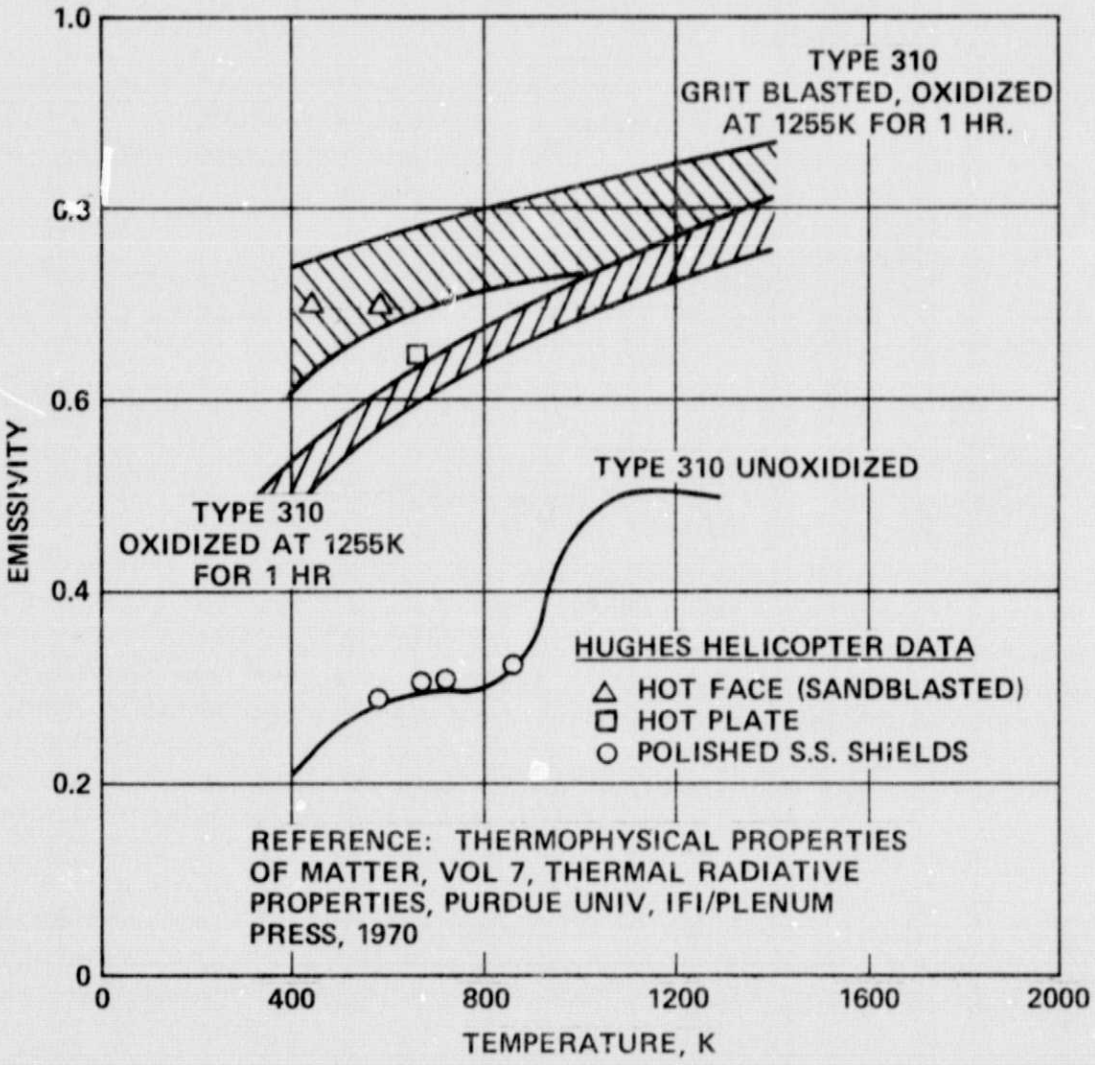

Figure 4.—Emissivity test results.

For the purpose of analysis and design, it was initially assumed that the foil radiation shield had an emissivity of 0.7. Subsequent data showed that the emissivity was closer to 0.35 making the insulation more effective.

A previous program conducted by Hughes at private expense resulted in a breakthrough in high temperature, low emissivity, radiation barrier technology. Gold coated Type 301 stainless steel foil samples were tested in ambient air at standard pressure and 1144 K for 1026 hours without failure and with exceptional retention of gold luster. Emissivity values were in the range of 0.04 to 0.10 prior to heating, and were unchanged after 46 hours of exposure at 1144 K.

Oxidation Tests

Type 304 stainless steel materials were oxidized in still air and air at a velocity of 45.7 m/sec. The materials demonstrated a high oxidation resistance without any evidence of the rapid oxidation (burning) observed with small diameter (less than 25 micron) filaments. The experimental results are shown in figure 5 for a range of temperature to 1273 K.

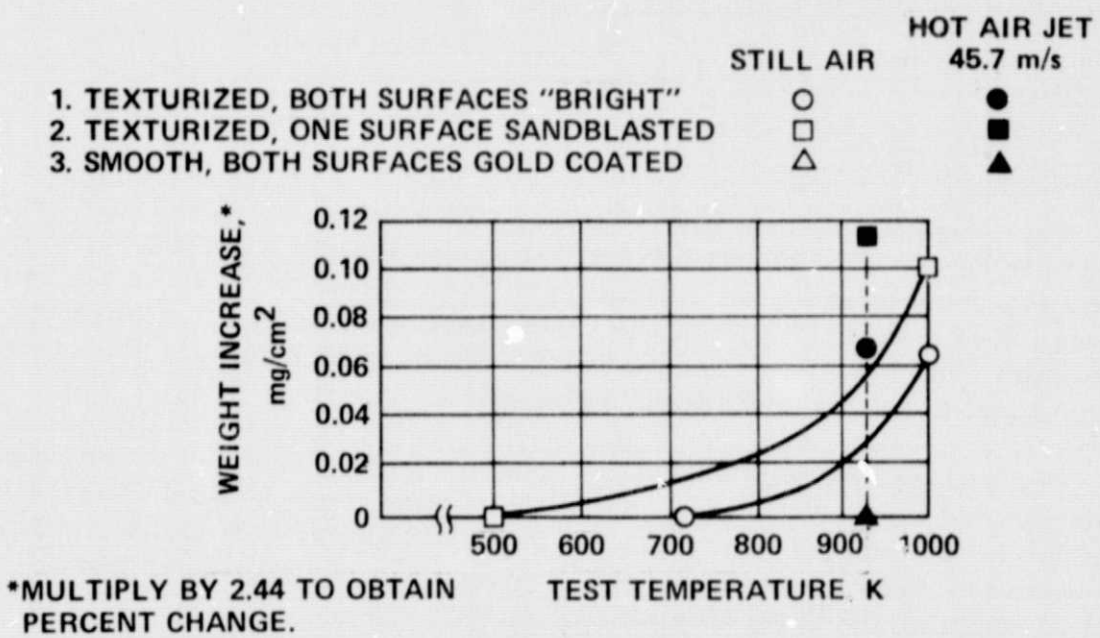

Figure 5.—Oxidation test results.

Structural Tests

The performance exhibited by four sample insulations, when subjected to mechanical load tests, is summarized in table 12.

TABLE 12. – SUMMARY OF STRUCTURAL TEST RESULTS

Specimen	Nominal Thickness	Initial Overall Thickness mm	Initial Internal Thickness mm	Internal Thickness* Under Design Load, mm	Weight Ratio,** Actual to Predicted	Comments
1	0.25	0.813	0.250	Zero	79%	No sides
2	1.02	1.321	0.762	0.076	79%	No sides
3	10.2	11.811	10.795	9.474	82%	Top perimeter folded to form box
4	10.2	11.252	10.693	9.449	78%	No sides

*Obtained from figure 6 by subtracting thicknesses of metal skins and shields.
**Based on table 12 (which does not include reduced weight of sandblasted surface).

The response of insulation samples to a uniformly applied load is presented in figure 6. The top third of the graph depicts a nominal 0.25 mm thickness (Specimen 1); the middle third of the graph illustrates the performance of a nominal 1.0 mm thick (Specimen 2); and the bottom third of the graph shows the data obtained with a nominal 10.2 mm thickness (Specimens 3 and 4, with and without "sides").

The reduced performance of Specimens 1 and 2 was due to too sparse a "conebutton" population. A comparison of Specimens 3 and 4 shows that the "sides" of the boxes do not significantly influence the test results. Sample 2 experienced a dip in the compressed thickness characteristics which resulted from exceeding the structure elastic limit.

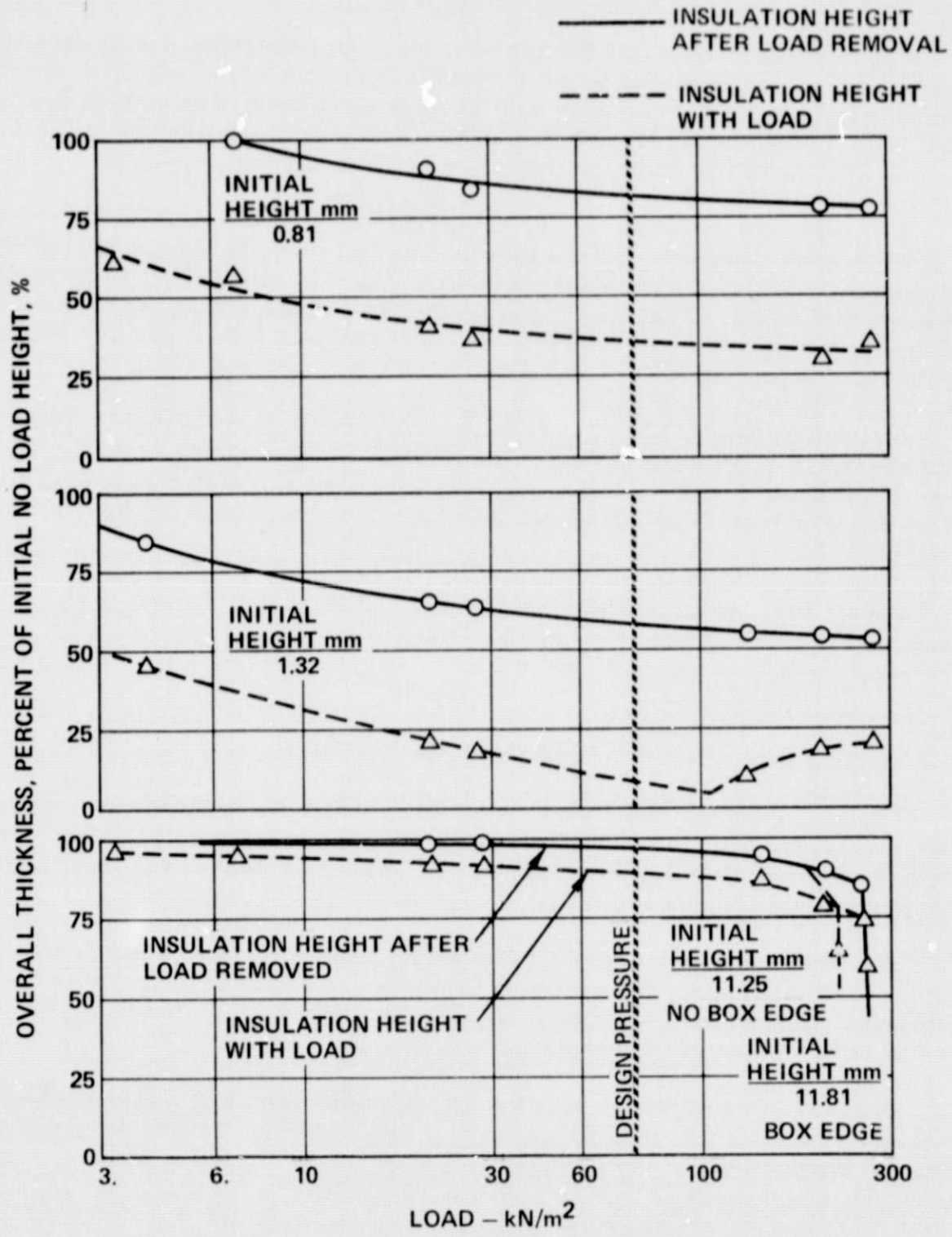

Figure 6. – Load capacity of LOW-Q type S-1 insulation.

Erosion/Impact Tests

The thinnest (1 mm) and the thickest (12 mm) insulations, were tested at two impact angles in two different environments; rain and sand. The rain concentration was 2.54 cm/hour with an average droplet size of 1950 microns. The droplet size ranged from 2375 to 595 microns with 74 percent in the 1800 to 2100 micron range. Impact velocity was 515 km/hour.

The sand concentration was 0.34 mg/cm^3 with an average particle size of 370 microns compared to the more ususal test particle size of 200 microns. An impact speed of 515 km/hour was used, which is comparable to tests in references 5 and 6. The rain concentration was equal to that used in the reference tests; however, the sand concentration was four times greater, to duplicate previous Hughes experience.

A photograph of the Hughes erosion test facility is presented in figure 7. The results of tests performed in this facility are given in figure 8; results from references 5 and 6 for non-metallic insulations are also shown for comparison. The metal insulation was superior to the non-metallic by a wide margin.

Except for the uniform abrasion of the surfaces, neither the rain nor the sand caused any damage and there was no evidence of deformation or cracking.

Thermal Conductivity Tests

Thermal conductivities were determined using the hot plate test apparatus shown schematically in figure 9. The five (5) configurations selected from the study were evaluated at various insulation temperatures and the test results are presented in figure 10.

The three thinner insulations duplicate the LOW-Q performance shown in figure 1. Higher average insulation temperatures were not run due to test equipment limitations; however, conductivity data extrapolated from 673 K to 700 K falls within predicted levels.

Test results with the 10 mm thick insulation which had three (3) stainless steel radiation shields (configuration 5) closely agreed with the predicted thermal conductivity.

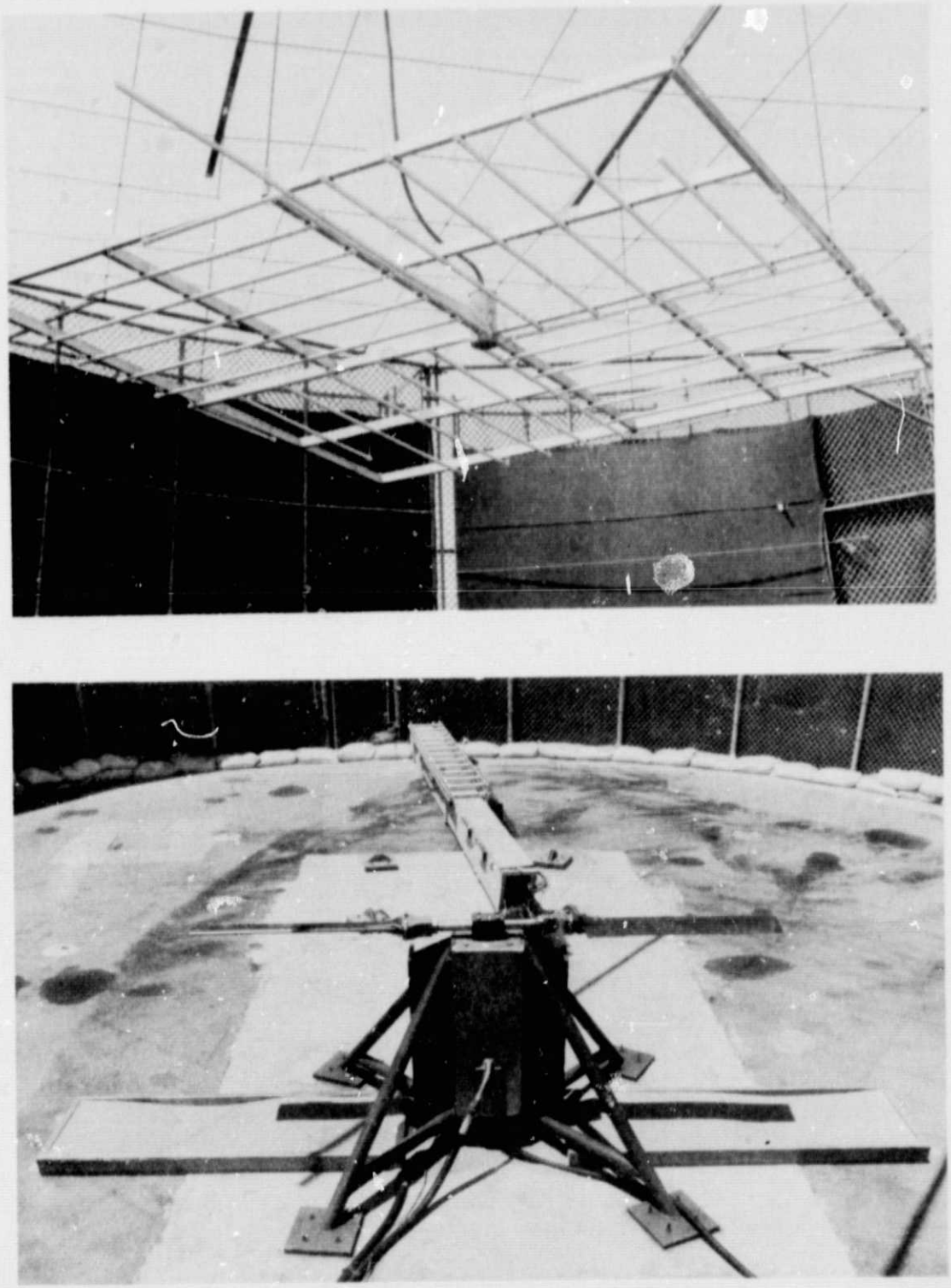

Figure 7.–Hughes' rain/sand erosion test stand.

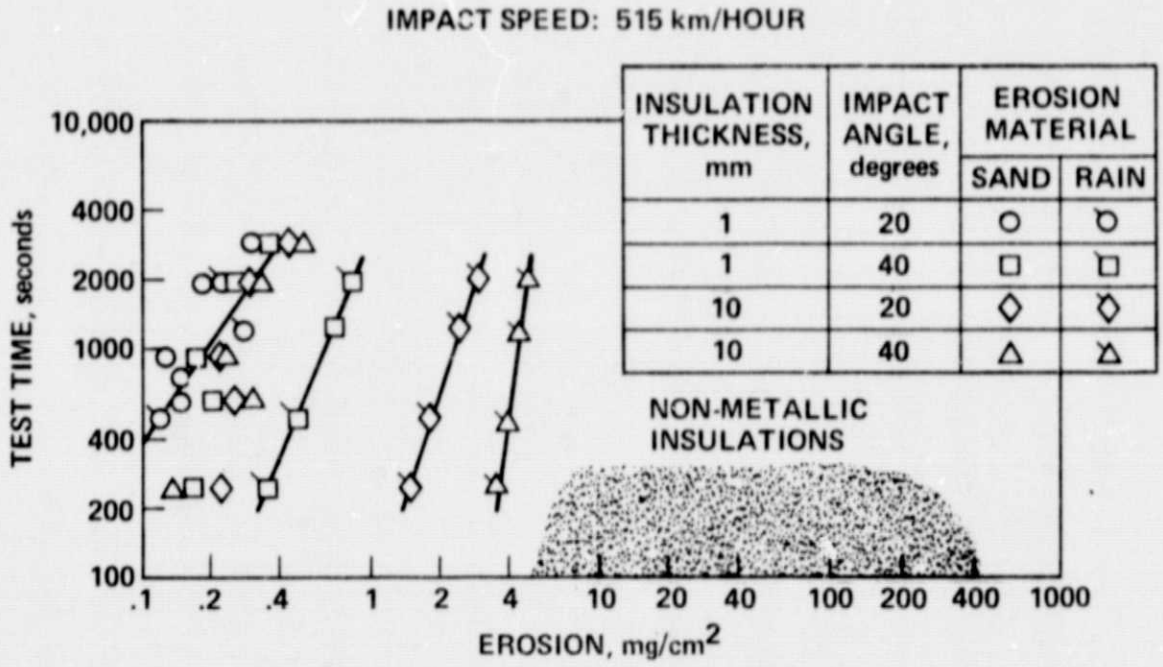

Figure 8.–Results of rain or sand erosion tests.

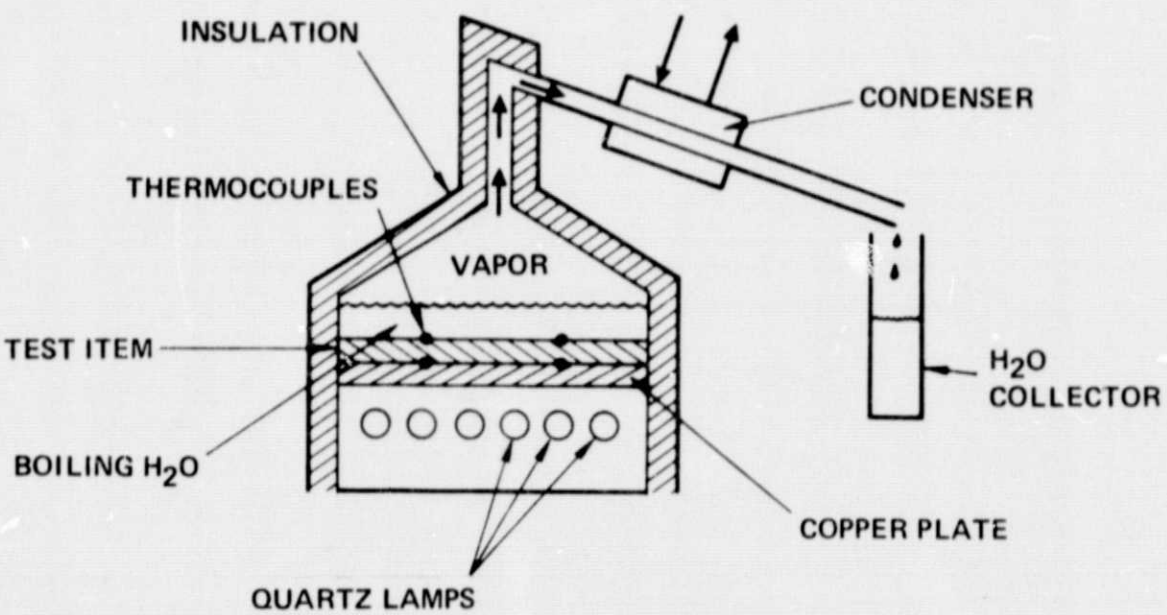

Figure 9.–Thermal conductivity test apparatus.

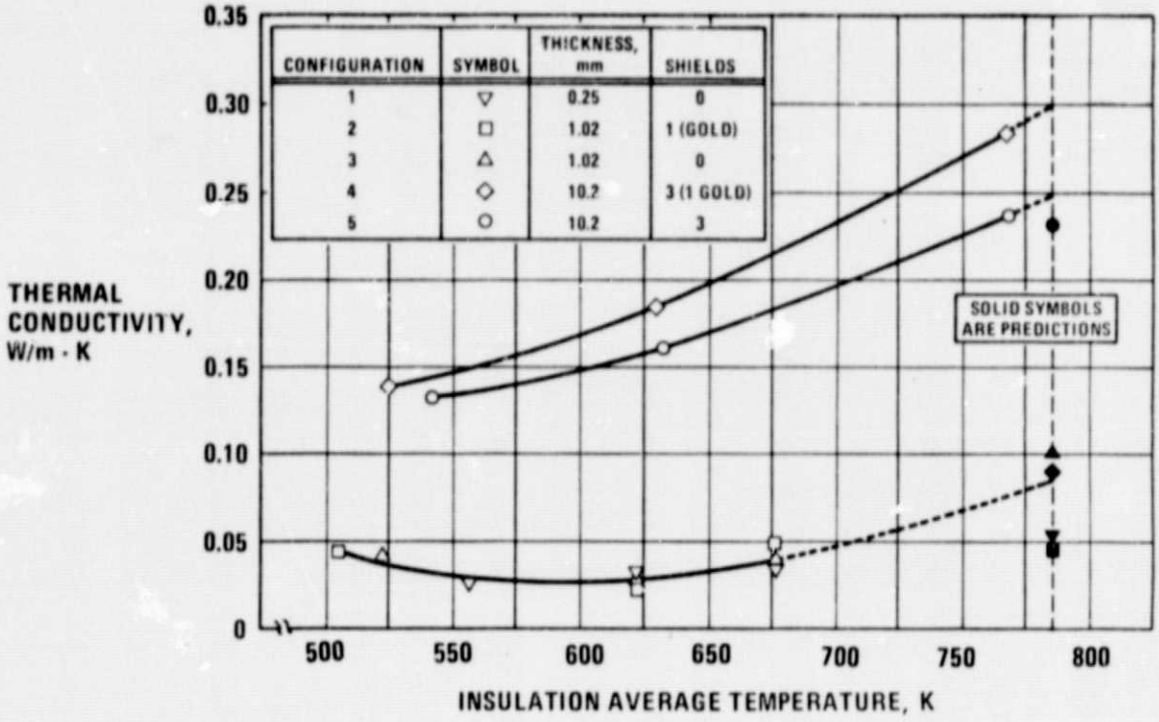

Figure 10.—Thermal conductivity test results.

Radiant heat represents 75 percent of the total heat transferred through Specimen 5 configuration and test data for Specimen 5 were very close to analytical predictions with higher emissivity ($\epsilon = 0.70$) shields. An improvement in thermal insulation is therefore expected if lower emissivity radiation shields are used.

The same configuration with one gold and two stainless steel shields exhibited a higher thermal conductivity, which was contrary to the expected trend. Subsequent disassembly of this test panel showed that inadequate clearance between the middle radiation barrier and the conebutton supports permitted a thermal short whose effect was greater than the benefits attained with one gold radiation shield.

Samples for Hypervelocity Tunnel Test

Ten specimens, each equipped with chromel-alumel thermocouples, were delivered for testing by the Langley Research Center. A photograph of the three samples, each of a different thickness, is presented in figure 11. Results of the tests will be reported by NASA at a later date.

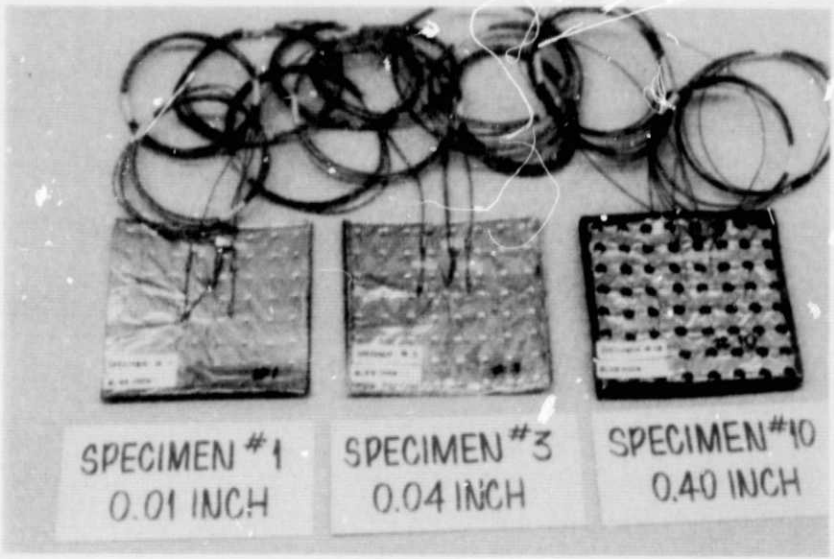

Figure 11.–Representative specimens of the three insulation thicknesses.

Structure is provided by "conebuttons" formed integral with the ba sheet for very thin insulation and by conebutton strips for the thicker insulation.

INSTALLATION ON AN AERODYNAMIC SURFACE

General Considerations

The attachment of insulation to the aircraft surface may be arbitrarily treated for two cases; (Case I) attachment to an existing aerodynamic surface and, (Case II) a new aircraft where insulation thickness may vary internally from a selected aerodynamic face.

Case I - Attachment to an existing airfoil surface.–The Case I installation restricts attachment options and would not be expected to permit weight optimization by modification of the basic airfoil surface. Attachment to the surface for this type of installation is generally limited to bonding systems such as RTV.

Case II - Attachment to a new aircraft.—A new aircraft (Case II) allows the thermal protection system design to be integrated in the basic structural system. Metal insulation, for example, is required to carry aerodynamic loads which in turn may be transferred to structural members directly. An aircraft "skin" under the thermal protection system is not required.

Mechanical attachment means are practical when a new airframe is being designed. Wing structure may be configured to accept sections of insulation which may be removed for servicing, or replaced if defective. The definition of specific mechanical attach systems is beyond the scope of this study; however, it is judged that innovative design can readily identify practical systems.

Venting of Insulation

Venting may be accomplished by either a lateral venting to the insulation blanket (or tile) perimeter, or by a manifolding of sections of insulation to a common vent point. The design for venting is intimately related to the aircraft application, i. e., the local static pressure differences that occur, the pressure load for which the skin is designed, aircraft structure, etc.

The insulation is designed to be vented within itself in all dimensions; therefore, venting to a selected ambient pressure will be at the discretion of the designer when application is being made to an aircraft. Several possibilities are shown in figure 12.

Joining of Adjacent Insulation Sections

The ten different joint configurations presented in reference 1 were reviewed before arriving at a recommended design for the "conebutton" fastening system. The rationale for selection included:

1. Thermal shorts
2. Complexity
3. Aircraft installation
4. Cost
5. Reliability
6. Maintenance and repair

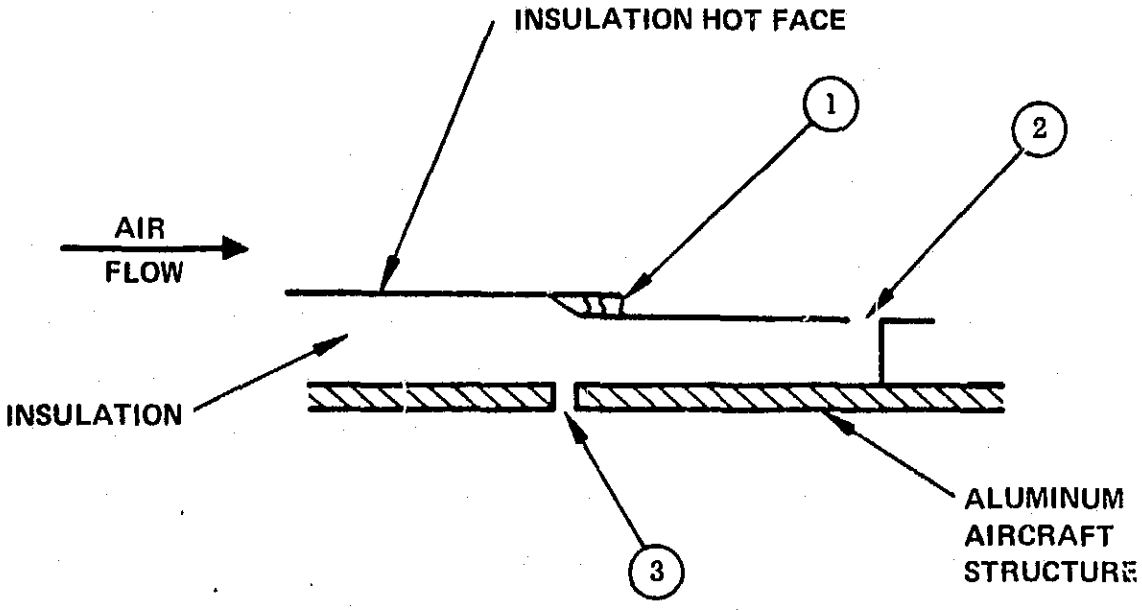

Systems Shown

(1) Shingle Design Weld Porous Plug Of Reticulated Stainless Steel Foam In Position To Maintain Skin Continuity Of Structure

(2) Vent Low Points Of Insulation Sections Upward To Static Environment

(3) Vent Insulation Sections To Inside Of Structure. Direct To Discrete Locations Or Otherwise Control Static Pressure

Figure 12.—Venting concepts for metal insulation systems.

The conebutton fastening system inherently provides a local containment of hot face thermal expansion; therefore, special provisions for joints are unnecessary for thermal growth. A vertical butt joint with the blanket (tile) edges sealed as required for venting is acceptable from both structural and thermal short considerations. An overlap of the outer (hot) skin is an optional feature which may be added to reduce gas circulation in the joint and the entrance of moisture or foreign matter.

The recommended design is a butt joint, optionally shielded by an overlap of metal skin similar to or an extension of the outer skin of the insulation.

PRODUCTION COSTS

A production cost estimate based on 1975 dollars was made for 465 square meters of all-metal insulations. The costs are summarized and compared with other heat shield costs in table 13. The costs include quality control and packaging for shipment.

LOW-Q insulations were judged to cost less than $2400 per square meter.

TABLE 13. – INSULATION PRODUCTION COST ESTIMATES

Insulation Reference		$/m^2$
Hughes Helicopter LOW-Q Type S-1 in Current Program	1	753
	2	1,184
	3	753
	4	2,367
	5	1,937
Hughes Helicopters LOW-Q Type W NAS CR-132389		1,775
NASA TMX-2719 Martin MAR-S1		3,228
NASA TMX-2570 Ablators		1,345

CONCLUSIONS

An all-metal surface insulation, developed for use over the actively cooled structure of a proposed hypersonic cruise vehicle, has been fabricated from 300 series stainless steel in thicknesses of 0.8 to 12 mm to meet the design objectives for very thin insulation packages fabricated from state-of-the-art alloys. The insulation consists of a 0.127 mm thick outer skin, textured to accommodate thermal expansion, and oxidized to achieve high emittance; a conical foil internal support system; and foil radiation shield insulation spaced within the package.

The results of environmental tests on laboratory samples of the insulation can be summarized as follows:

1. Metal insulation thermal conductivity, measured at atmospheric pressure and 800 K, was in the same range as the thermal conductivity of reusable surface insulation, the space shuttle baseline TPS (figure 1).

2. The metal insulation was resistant to rain and sand erosion, experiencing only uniform abrasion without any evidence of deformation or cracking. The greatest erosion, 5 mg/cm^2, occurred after exposure in rain for 2000 seconds at 2.54 cm/hr, a velocity of 515 km/hr, and a 40-degree impact angle (figure 8).

3. The metal insulation was resistant to oxidation, experiencing no more than 0.3 percent weight gain after 30 minutes exposure to flowing air at 1220 K (figure 5).

4. The production cost of the metal insulation has been estimated to be less than \$2400/m^2, which is competitive with the cost of the space shuttle reusable surface insulation (table 13).

RECOMMENDED APPLICATIONS

The current study successfully defined and substantiated a thermally efficient structure for packaging all-metal heat shields for hypersonic vehicle applications where temperatures do not exceed 1200 K. This insulation has other areas of application, such as:

- Lifting body insulation
- Hot gas blown wings (STOL)

- YF-12 extended high speed aircraft
- Space shuttle orbiter surfaces
- IR suppression for exhaust tailpipes

RECOMMENDED STUDIES

To demonstrate the full capabilities of all-metal insulation a two phase program should be continued, extending to flight test. The two phases and subtasks would include:

Phase I - Insulation R&D

- Evaluate vehicle attachment methods
- Demonstrate fatigue life
- Develop conebutton fabrication

Phase II - Applications

- Manufacture production size pieces
- Install on aircraft
- Flight test

APPENDIX A

STRUCTURAL DESIGN ANALYSIS

APPENDIX A

STRUCTURAL DESIGN ANALYSIS

1.0 SUMMARY

1.1 Parametric Analysis

Studies were performed to provide design tools for the selection of insulation configurations. Supports for a skin thickness of 0.127 mm were defined for a pressure load of 1.38 kN/m^2, which was selected to act internally to place all welded joints in tension. This was judged to be the most severe structural loading that should be expected on the planform of a hypersonic aircraft.

1.2 Skin Support

A rectangular spacing was selected because other spacing geometry was not found to offer an advantage over rectangular system. A conical sheet metal "conebutton" was selected to provide structural and dimensional integrity.

The support population required to carry 1.38 kN/m^2 skin load is analytically shown in Appendix B to give a 3.8 percent thermal short based on constant diameter supports. The thermal short is 6.2 percent when corrected for the conical support shape.

1.3 Configuration Structure and Rationale

a.	Outer skin thickness:	0.127 mm 300 series stainless steel for all insulation systems
b.	Aerodynamic negative pressure difference:	1.38 kN/m^2
c.	Outer skin deflection:	0.254 mm (thickness of minimum insulation)
d.	Support spacing:	15.24 mm (figure 13)
e.	Support population:	4300/m^2
f.	Weld joint diameter:	0.242 mm (figure 14)

g.	Conebutton wall:	0.0254 mm minimum (to take 1.38 kN/m^2 structural loads)
h.	Conebutton apex:	3.175 mm (for entry of welding electrode)
i.	Conebutton angle:	25 degrees (for common fabrication)
j.	Insulation thickness range:	0.25 to 10.16 mm
k.	Maximum conebutton base/apex area ratio:	2.5 (for maximum insulation)
l.	Q/K thermal short correction factor:	1.64 (page 41)
m.	Maximum change in insulation thermal conductivity:	6.2 percent
n.	Initial k:	0.115 W/m · K from Appendix B
o.	Modified k:	0.122 W/m · K (corrected for 6.2 percent)

2.0 ANALYSIS AND DESIGN

2.1 Skin Deflection

Deflection was analyzed for a 0.127 mm thick infinite metal plane and a parametric solution was defined for a range of aerodynamic loads and a rectangular spacing of coordinates. The analysis is described as follows, based on equations from reference 7.

The skin deflection is:

(1) $\omega = qb^4/384D$

$$- \frac{qa^3b}{2\pi^3 D} \sum_{m=2,4,6}^{\infty} (-1)^{m/2} \frac{Xm + \tanh Xm}{m^3 (\sinh x_m \tanh x_m)}$$

$$- \frac{qa^3b}{2\pi^3 D} \sum_{m=2,4,6}^{\infty} \frac{Xm - \dfrac{Xm + \tanh Xm}{\tanh^2 Xm}}{m^3}$$

This is simplified in reference 7, by use of a tabular solution of $x = f(b/a)$ to

(2) $\omega = x_b^4 q/D$

where

q = uniform loading, 1.380 kN/m^2

D = $Eh^3/(1 - \nu^2)$ = 0.32778

E = 200 GN/m^2 S. S. 300 series

ν = 0.28 Poisson's Ratio

h = 0.127 mm plate thickness

x_m = $m\pi b/2a$ dimensionless,
a and b are shorter and longer sides of rectangular array, mm

ω = deflection, mm

Insertion in the foregoing values in equation (2) gives:

(3) $\omega = 3.72 \times 10^{-4} xb^4/D$

The solution of (3) is presented in figure 13 for a range of support spacing and resultant deflection to provide a parametric design tool for application in specific design. For a support spacing of 15.24 mm, the design load will deflect the skin less than 0.254 mm, which is less than the thickness of the thinnest insulation. This corresponds to a population density of 4300 welds per square meter.

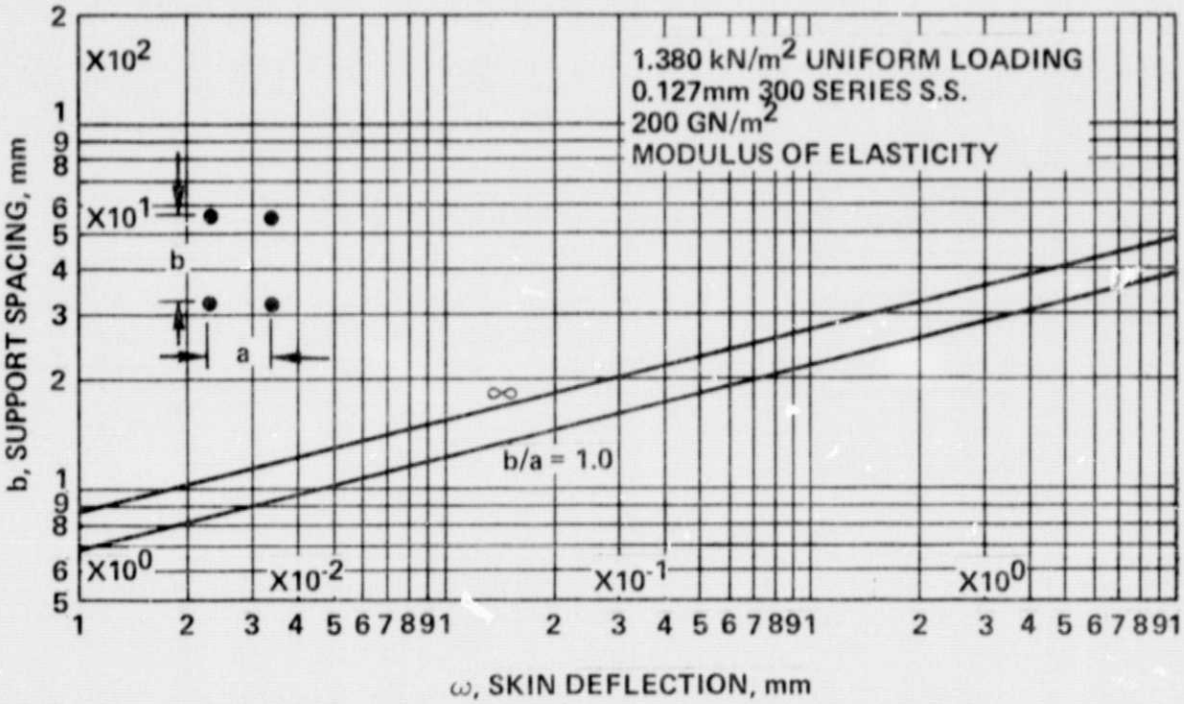

Figure 13.—Skin deflection variation with support spacing.

2.2 Skin Weld Support Area

The weld diameter for support of the skin in a negative pressure mode (which places the weld in tension) is defined in the following manner:

(1) $f_t = P_2 \, ab/A_w$

and

$$(2)\quad d = (4P_2 ab/\pi f_t)^{0.5}$$

where

f_t = weld allowable* tensile strength, 68.95 MN/m^2

P_2 = negative pressure differential, MN/m^2

a = support spacing, mm

b = support spacing, mm

d = diameter of metal weld, mm

A_w = area of metal weld, mm^2

(*reference 7)

Equation 2 is charted in figure 14 and illustrates the range of spacing and weld area combinations that satisfy the structural load requirements imposed on the weld itself. The 15.24 mm square spacing requires a weld area of 0.242 mm diameter for structural integrity with a gas load of 1.38 kN/m^2.

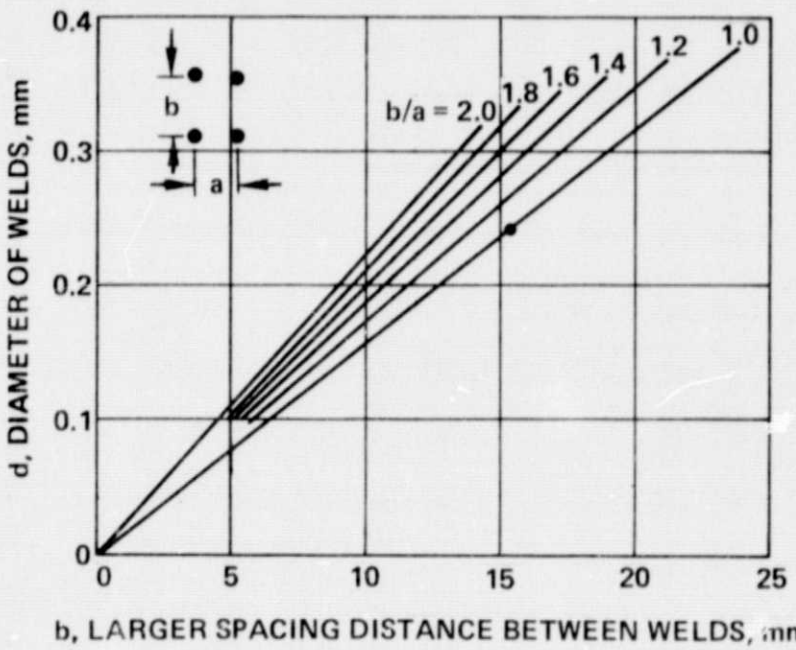

Figure 14.—Support spacing variation with attach point diameter.

2.3 Conebutton Metal Thickness and Configuration

The thickness of metal required (in tension) to accommodate a 1.38 kN/m^2 skin gas load is 0.0254 mm, based on the following criteria:

a. Apex of conebutton = 3.175 mm (to allow entry of weld electrode)

b. Allowable tensile strength - 68.95 MN/m^2

c. Size of weld attachment (weld nugget) = 0.242 mm diameter

d. Support population = 4300 welds per square meter

The column load carrying capability of a hollow cone support is in excess of its tensile load capability, based on an analytical inspection.

Metal 0.0254 mm thick was used in the conebutton fabrication. The total conical angle was 25 degrees for ease in fabrication. A thicker metal may be necessary for forming of cones higher than 10 mm.

2.4 Conebutton Thermal Short

A correlation was performed to combine the interrelated effects of:

- Insulation thickness (conebutton height)
- Weld nugget area at skin (heat input area)
- Geometry of hollow cone sheet metal supports (conebuttons)

The analysis was performed to determine a factor which could relate the thermal short of a hollow conical support to that of a solid metal column (such as a wire). The solution for the thermal short increase of a conebutton support is presented below. The term Q/K is the multiplier to be applied to a cylindrical column thermal short system.

(1) $Q = -k A \, dT/dx$

(2) $A = A_o + ax$ where $a = (Ab - Ao)/\ell = (A - Ao)/x$

(3) $A_b = Ao + al = \pi d_b h$

(4) $-kdT = Q \frac{dx}{Ao + ax}$

(5) $-k \int_{To}^{Tb} dT = Q \int_{X_o}^{X_b} \frac{dx}{Ao + ax}$

(6) $-k(T_b - To) = \frac{Q}{a} \ell n \left(\frac{Ao + aX_b}{Ao + aXo} \right)$

(7) $= \frac{Q}{a} \ell n \left(\frac{A_b}{Ao} \right)$

(8) $= \frac{Q}{a} \ell n\ n$ where $n = A_b / Ao$

(9) $\frac{Ab}{Ao} = \frac{Ao + a\ell}{Ao} = 1 + \frac{a}{Ao} \ell = n$

(10) $a = (n - 1)Ao/\ell$

(11) $-k(T_b - To) = \frac{Q}{(n - 1)\ Ao} \ell n\ n$

(12) Then $\boxed{\frac{Q}{K} = \frac{(n - 1)}{\ell n(n)}}$ where $K = -k(T_b - To)Ao/\ell$

The thermal short factor (Q/K) is 1.64, for example, for the thickest insulation. Analysis made in Appendix B indicates a basic change in insulation thermal conductivity of 3.8 percent. The conebutton modifies this to 6.2 percent. Thus the insulation thermal conductivity of 0.115 W/m · K, from Appendix B, is increased to 0.122 W/m · K.

APPENDIX B
THERMAL SHORT ANALYSIS

APPENDIX B

THERMAL SHORT ANALYSIS

Thermal shorts created by connecting "wires or welds" were investigated based on the parameters in table 16.

TABLE 16. – MATERIAL THERMAL CHARACTERISTICS

Item	Parameter	Selected Value
1	Average insulation thickness	7.62 mm
2	Average insulation temperature	846 K
3	Thermal conductivity of LOW-Q$^{(tm)}$ insulation	0.115 W/m · K Reference 1
4	Thermal conductivity of 300 series stainless steel	22.2 W/m · K Reference 1

The respective heat transfer coefficient for a 7.62 mm thickness are:

LOW-Q insulation: $h_i = kx^{-1} = 0.115/0.00762 = 15.1\ W/m^2 \cdot K$

Stainless steel: $h = kx^{-1} = 22.2/0.00762 = 2913\ W/m^2 \cdot K$

Effect of Weld Population on Insulation Thickness

The number of small welds or mechanical connections per unit area was found to have a secondary effect in the insulation system design, as explained by the following analysis:

Let N be the number of welds per square meter. Then the fraction of surface devoted to welds is NA_N, where A_N is the area (meter^2) of each weld nugget.

A thermal insulation with thermal shorts (h_t) has to be thicker (x_t) to product the same insulation as one without thermal shorts.

Thus:

$$h_t = (k_i + NA_N k_{ss})/x_t$$

or

$$x_t = (0.115 + NA_N 22.2)(k_i/x)^{-1}$$

Therefore:

$$x_t/x = (0.115 + NA_N 22.2)/0.115 = 1 + 192.5\ NA_N$$

and the percent increase in insulation thickness = $19,250\ NA_N$.

Thus for typical 0.242 mm diameter weld nuggets, a weld population of 4300 welds per square meter affects the insulation thickness by only 3.8 percent.

REFERENCES

1. NASA CR-13289, "Metal-Wool Heat Shields for Space Shuttle," Robert C. Miller and John L. Clure, Hughes Helicopters, March 1974.

2. NASA SP-7012, "The International System of Units," E. A. Mechtly, 1973.

3. Hughes Helicopters Report HH 75-18, "Rapid Oxidation (Combustion) of Steel and Stainless Steel Filaments," R. C. Miller and G. R. Ranslem, February 1975.

4. Thermophysical Properties of Materials, Volume 7, Thermal Radiative Properties, Purdue University, IFI/Plenum Press, 1970.

5. AD 750793 (AFML-TR-72-145), "Rain Erosion Characteristics of Thermal Protection System Materials at Subsonic Velocities," Bell Aerospace Company, August 1972.

6. AD 879462 (AFML-TR-70-265), "Supersonic Rain and Sand Erosion Research: Erosion Characteristics of Aerospace Materials," Bell Aerospace Company, November 1970.

7. Timoshenko & Wainowsky-Drieger, "Theory of Plates and Shells."